ACS APPLIED MATERIALS & INTERFACES

Letter

www.acsami.org

Reversible Switch between Bulk $MgCO_3 \cdot 3H_2O$ and $Mg(OH)_2$ Micro/Nanorods Induces Continuous Selective Preconcentration of Anionic Dyes

Yongjing Wang, Jingping Chen, Lili Lu, and Zhang Lin*

†State Key Laboratory of Structural Chemistry, Fujian Institute of Research on the Structure of Matter, Chinese Academy of Sciences, Fuzhou, Fujian 350002, China

Supporting Information

ABSTRACT: It is still a big challenge to treat large amount of water with low concentration of pollutant. In this study, a hierarchical (micro/nano) structured $Mg(OH)_2$ adsorbent was introduced by the in situ hydration of porous MgO in the dye solution. The adsorbent showed high selective adsorption capacity ($Q_0 \approx 155$ mg/g for acid alizarine blue) and fast adsorption rate for the removal of anionic dyes down to the mg/L levels. Moreover, the adsorbed dye was successfully desorbed by carbonation, resulting in a ~4000 fold enrichment of the dye solution. It was demonstrated that by establishing a reversible switch between the $Mg(OH)_2$ micro/nanorod and the bulk $MgCO_3 \cdot 3H_2O$, a continuous preconcentration of low-concentration dye wastewater could be achieved.

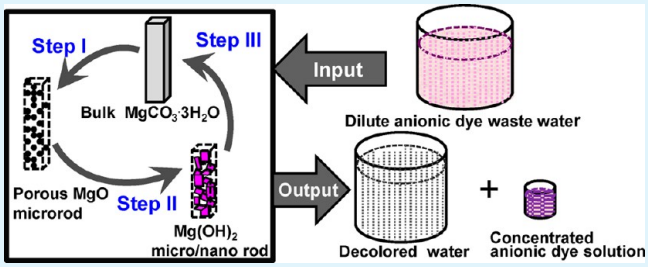

KEYWORDS: *$Mg(OH)_2$ micro/nanorods, dye wastewater, preconcentraion, selective adsorption, anionic dye, carbonation*

1. INTRODUCTION

Textile dye processes are among the major industrial water users. In some developing countries, the amount of wastewater discharged from the textile industry is estimated to be more than one billion tons annually.[1] To treat high-concentration dye wastewater, existing methods include coagulation, biodegradation, precipitation, and chemical oxidation.[2−8] However, even after treatment with the above methods, the water may still contain low concentrations (<10 mg/L) of soluble ionic dyes, which is visually characterized by incomplete decolorization. As a feasible and cost-effective method, the adsorption technique could be potentially applied to large-scale treatment of industrial wastewater. Conventional materials such as activated carbon, natural minerals, and industrial waste residue,[9−12] exhibit high adsorption capacity when used to treat high-concentration wastewater. However, these materials become ineffective in treating dilute dye wastewater, which could be attributed to the weak interface force between the organic waste and the conventional adsorbents. It is therefore necessary to develop a technique specifically for treating and completely decolorizing wastewater that contains dilute cationic and/or anionic dyes.

Nanomaterials are inherently superior adsorbents due to their high surface area and active adsorption sites. As demonstrated in our previous work, low-concentration substances in wastewater could be enriched after an adsorption/desorption cycle by adjusting the interface state of the nanoadsorbents.[13−15] The enriched solution can either be treated by conventional methods or used directly for industrial purposes. The preconcentration step requires that the adsorbent should possess high affinity toward the target pollutant. Moreover, the adsorbed pollutant could still desorb from the adsorbent when the interface force between the two is eliminated.

Guided by the above idea, we successfully developed a highly efficient ZnS:Cu adsorbent that was able to separate the cationic dye from the wastewater.[14] With this adsorbent, wastewater containing ~10 mg/L dye was concentrated more than 1000 times. The adsorption mechanism was believed to be the excess negative charge on the adsorbent surface capturing the cationic dye through electrostatic interaction. In this work, for the purpose of specifically treating the dilute ionic dye, we attempted to design a material with surface positive charge to adsorb and enrich the anionic dye.

As a nontoxic and environmentally friendly material, nano-$Mg(OH)_2$ has shown high adsorption efficiency to anionic pollutants.[16−19] In our previous work,[15] we demonstrated that dilute Cr(VI) could be removed by the nano-$Mg(OH)_2$ adsorbent. Specifically, the enrichment of Cr(VI) and retrieve of the adsorbent were simultaneously realized via the reversible transformation between nano-$Mg(OH)_2$ adsorbent and bulk $MgCO_3 \cdot 3H_2O$. However, only 40-fold enrichment was achieved for 5 mg/L Cr(VI) solution. In this work, we systemically investigated the influence of the MgO structure on

Received: June 19, 2013
Accepted: July 30, 2013
Published: July 30, 2013

the hydration and the adsorption performance of $Mg(OH)_2$. $Mg(OH)_2$ micro/nanorod with high adsorption capacity was obtained by fast hydration of the porous MgO microrod. The feasibility of its application in selective enrichment of low-concentration anionic dye solution was also investigated. The experimental design is shown in Scheme 1. With a reversible route between the hierarchical structured $Mg(OH)_2$ and bulk $MgCO_3{\cdot}3H_2O$, the dilute dye solution was completely decolored, and the anionic dye highly enriched. This new adsorbent enabled a continuous preconcentration of low-concentration dye wastewater.

Scheme 1. Recycling strategy for Treating Wastewater Containing Low Concentrations of Anionic Dyes[a]

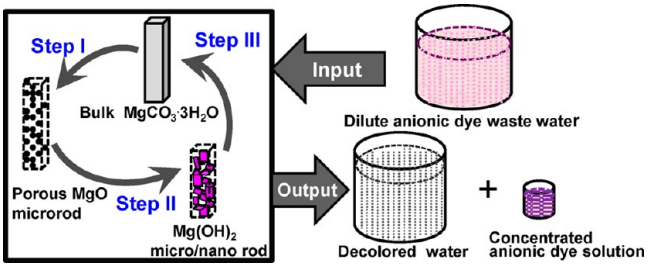

[a]Step I: Generation of MgO microrods by pyrolysis from bulk-$MgCO_3{\cdot}3H_2O$. Step II: Applying self-supported $Mg(OH)_2$ micro/nanorods to adsorb low concentrations of dye in the wastewater. Step III: Desorption and enrichment of the dye via the phase transformation from $Mg(OH)_2$ micro/nanorods to bulk $MgCO_3{\cdot}3H_2O$.

2. EXPERIMENTAL SECTION

2.1. Materials and Instruments. All of the chemicals were AR reagents obtained from commercial sources and used without further purification.

X-ray diffraction (XRD) was used to identify phase and crystal structure of the obtained samples. Diffraction data were recorded using a PANalytical X′ Pert PRO diffractometer with Cu Kα radiation (40 kV, 40 mA) in the continuous scanning mode. The 2θ scanning range was from 10° to 80° in steps of 0.03° with a collection time of 20 s per step. The BET surface area was determined by a multipoint BET method using adsorption data in the relative pressure (P/P_0) range of 0.05−0.25. A desorption isotherm was used to determine the pore size distribution by the Barret−Joyner−Halenda (BJH) method, assuming a cylindrical pore model. The SEM analyses were performed using a JSM-6700F equipped with an Oxford-INCA energy-dispersive X-ray (EDX) spectroscopy. A Shimadzu UV-2550 spectrophotometer was used to record the UV/vis spectra of various samples. HRTEM analyses were performed on a JEOL JEM2010 HRTEM instrument at 200 kV. The Zetasizer Nano ZS90 (Malvern Instrument) was used for the measurement of the zeta potential of the samples.

2.2. Preparation of MgO Microrods and the Self-Supported $Mg(OH)_2$ Micro/Nanorods. The $MgCO_3{\cdot}3H_2O$ microrods were first synthesized according to the reference.[20] Briefly, 10 g of commercial light-burned magnesium oxide was thrown into 50 mL deionized water. The mixture was heated at 90 °C for 1h. Then the solid were transformed to a cylindrical stainless steel vessel. The vessel was then sealed, with an opening connected to a CO_2 high-pressure bomb. The pressure of CO_2 was controlled at 0.5 M pa for 12 h at room temperature. The obtained colorless powder was collected for XRD analysis and SEM observation.

The MgO powders with different hydration properties were obtained by pyrolysis of $MgCO_3{\cdot}3H_2O$ at 600 °C for 1.5 h ($MgO_{600-1.5h}$), 3 h (MgO_{600-3h}), and 12 h ($MgO_{600-12h}$)), respectively. The $Mg(OH)_2$ micro/nanorods were prepared by the hydration of MgO microrods in water or the dye solution at the room temperature.

2.3. Adsorption Experiments. Two aliquots of $MgO_{600-1.5h}$ powder were put into the 2.5 and 5 mg/L acid alizarine blue (AB) solution, respectively. The dosage of the adsorbent was 1 g/L. The mixture was stirred for 1 h until the $Mg(OH)_2$ reached equilibrium with the dye. During this process, a sample of the supernatant (3 mL) was extracted for concentration analysis every 5 min.

The adsorption isothermal experiments were performed at room temperature. A set of AB solutions with concentrations ranging from 200 to 350 mg/L were prepared beforehand. Then, $MgO_{600-1.5h}$ (75 mg) was added to the dye solution (50 mL) that had been immersed in a water bath at 30 °C. After equilibrium, the concentration of the dye solution was determined by UV−vis spectroscopy.

Langmuir isotherm equation was adapted to fit the experimental data[21]

$$\frac{1}{Q_e} = \frac{1}{Q_0} + \frac{1}{C_e Q_0 b}$$

where Q_e is the amount adsorbed at equilibrium (mg/g) and C_e is the equilibrium concentration (mg/L). Q_0 is the maximum amount or the saturated adsorption amount (mg/g) and b is a constant related to the binding strength (L/mg).

Simulated mixed dye solutions were prepared to examine the selective adsorption performance of the adsorbent. Solution **1** contains Orange G (anionic, 10 mg/L), Rhodamine B (cationic, 5 mg/L), and Coomassie Brilliant Blue R-250 (anionic, 10 mg/L). Solution **2** contains orange IV (anionic, 15 mg/L), eosin B (anionic, 5 mg/L), and methylene blue (cationic, 5 mg/L). UV−vis spectra were determined before and after the adsorption.

2.4. Preconcentration of Low-Concentration Dye Solution. $MgO_{600-1.5h}$ powder (1.8 g) was put into a simulated wastewater sample (50 L) containing 5 mg/L AB. The mixture was stirred for 1 h until the $Mg(OH)_2$ reached equilibrium with the dye. The dye-loaded $Mg(OH)_2$ was then filtered out by vacuum filtration for further desorption and enrichment treatment. Then the $Mg(OH)_2$ sludge was treated by the carbonation method as described above. The concentrated dye solution was separated for UV−vis analysis. The sediment was then rinsed with distilled water 3 times. The solid product was reserved for the regeneration treatment.

2.5. Zeta Potential Measurement. The zeta potentials during the hydration process of MgO microrods were measured at 25 (±1) °C to explore the adorption mechanism. $MgO_{\_600\_1.5h}$ powder (0.01 g) was first put into 50 mL deionized water. The mixture was stirred for 1 h until it was totally transformed to $Mg(OH)_2$. During this process, 1 mL of the mixture was drawn for zeta potential measurements every 15 min.

3. RESULTS AND DISCUSSION

In the dye removing process, MgO precursor, obtained by heating $MgCO_3{\cdot}3H_2O$, was put into the low-concentration dye

solution to simultaneously generate $Mg(OH)_2$ adsorbent and adsorb the dye. The design ensures the following transformations.

$$MgCO_3{\cdot}3H_2O(\text{microrod}) \rightarrow MgO(\text{porous microrod})$$

$$MgO(\text{porous microrod}) \rightarrow Mg(OH)_2(\text{hierarchal micro/nanorod})$$

The experimental conditions for the preparation of the $Mg(OH)_2$ adsorbent are listed under Table 1. The $Mg(OH)_2$ with the highest adsorptive capacity was acquired by the hydration of $MgO_{600-1.5h}$. XRD and SEM were utilized to characterize the structure and morphology of the phases involved in the above process. As shown in Figure 1, after heating at 600 °C for 1.5 h, the $MgCO_3{\cdot}3H_2O$ phase was completely transformed to MgO. The size of MgO primary particles was calculated to be ~11.6 nm according to the Scherrer equation. SEM observation revealed that the morphology of MgO still preserved the skeleton of the $MgCO_3{\cdot}3H_2O$ microrods with the size up to 20 μm. The structure details of the MgO microrods were further imaged by the TEM. Meso pores were clearly seen in an individual MgO microrods. The HRTEM showed that the size of the primary nanoparticles was ~10 nm (more details see Figure S2 in the Supporting Information), which was consistent with the XRD results. On the basis of these data, it was implied that the MgO phase probably possessed a porous structure consisting of ~10 nm primary particles. Figure 1b shows the XRD pattern of the hydration product of the porous MgO. It indicates that MgO was totally transformed to $Mg(OH)_2$ after hydration. According to the (001) peak broadening, the size along [001] direction is ~10 nm. SEM observation revealed that the formed $Mg(OH)_2$ was rodlike aggregates, which consisted of 100−200 nm nanolamella. The micro/nanostructure of the adsorbent not only ensures adequate adsorption of the pollutants but also avoids aggregation and clogging problems that nanomaterials frequently encounter.

Table 1. Experimental Conditions and Adsorption Performance for $Mg(OH)_2$ Adsorbent[a]

sample	annealing temperature	size (nm)	BET surface area (m^2/g)	MgO% after 0.5 h hydration	MgO% after 1 h hydration
$MgO_{600-1.5h}$	600 °C for 1.5 h	8.9	82.1	31	0
MgO_{600-3h}	600 °C for 3 h	58	25.34	72	48
$MgO_{600-12h}$	600 °C for 12 h	>100	16.65	88	70

sample	C^b/C_0^c after 0.5 h hydration (%)	C/C_0 after 1 h hydration (%)	adsoption capacity (mg/g)
$Mg(OH)_{2\ 600-1.5h}$	100	100	155
$Mg(OH)_{2\ 600-3h}$	48	70	109
$Mg(OH)_{2\ 600-12h}$	28	50	52

[a]The size and phase content were calculated according to the XRD data, see Supporting Information, page S1. MgO samples were obtained by the pyrolysis of $MgCO_3{\cdot}3H_2O$ at 600 °C. $Mg(OH)_2$ samples were obtained by the hydration of the resulted MgO in the dye solution. [b]The concentration of the AB solution. [c]The original concentration of the AB solution (5 mg/L). The dosage of the adsorbent was 1 g/L.

To test the adsorption performance of the $Mg(OH)_2$ micro/nanorods to low concentrations of dyes in wastewater, we chose the simulated wastewater containing 5.0 or 2.5 mg/L AB solution. As shown in Figure 2, in the initial stage, the adsorption rate was extremely high. About 90% of the dyes were adsorbed in the first 10 min. The solution was completely decolored after 30 min. This showed high efficiency of the adsorbent for removing dyes from wastewater. The modeling of the experimental data reveals that it could be well fitted with the pseudo-second-order rate equation, suggesting that the rate-limiting step may be chemisorptions. The adsorption isotherm measured at 30 °C revealed that the adsorption behavior followed the Langmuir isotherm closely. After curve fitting, the Langmuir capacity (Q_0) and affinity constants (b) for $Mg(OH)_2$ were found to be 155 mg/g and 1.65 L/mg, respectively. The high Q_0 and b value indicated that the adsorbent possessed excellent adsorption ability and was suitable for large-scale wastewater treatment for wastewater containing low concentrations of dyes.

As mentioned before, whether cationic and anionic dyes could be selectively separated is one of the crucial factors for the reuse of the dye. To verify the selectivity of the $Mg(OH)_2$ adsorbent, it was applied in simulated wastewater containing mixed cationic and anionic dyes. As shown in Figure 3a, the peaks located at 475, 554, and 625 nm in the UV−vis spectra of solution **1** could be assigned to the characteristic adsorption of Orange G (anionic), Rhodamine B (cationic), and Coomassie Brilliant Blue R-250 (anionic), respectively. After adsorption, the characteristic peaks of the anionic dyes disappeared, whereas that of the cationoic dye changed only slightly. For solution **2**, which was composed of Orange VI (anionic), eosin B (anionic), and methylene blue (cationic), similar adsorption behavior was also observed. As shown in Figure 3b, only the characteristic peak of cationoic dye remains unchanged, those of the two anionic dyes disappeared. Therefore, it can be concluded that $Mg(OH)_2$ micro/nanorods is capable of selectively adsorbing low concentrations of anionic dyes in wastewater.

Then we examined the enriching properties of the adsorbent. Figure 4 shows that 50 L 5 mg/L AB solution was completely decolored with 2.5 g $Mg(OH)_2$ adsorbent. The dye loaded nano-$Mg(OH)_2$ solids that were in deep violet color was subsequently filtered out for further desorption measurement. Phase transformation was employed to achieve the goal of desorbing the anionic dye. After treatment at 0.5 MPa CO_2 for 12 h, $Mg(OH)_2$ micro/nanorods completely changed into bulk $MgCO_3{\cdot}3H_2O$ crystals. Meanwhile, deep violet dye solution was obtained (Figure 5c). The concentration was up to 20000 mg/L, which represented a nearly 4000-fold enrichment. The desorption of the dye could be ascribe to the reduction of the surface area from 72 $m^2\ g^{-1}$ for $Mg(OH)_2$ micro/nanorods to 3.2 $m^2\ g^{-1}$ for $MgCO_3{\cdot}3H_2O$. In addition, it was easy to extract the concentrated dye supernatant since the size increase of the magnesium compounds facilitated the settlement of the solids. According to the volume and concentration, it was estimated that the transformation lead to ~95% desorption of the dye. After regeneration by pyrolysis described before, the light grayish $MgCO_3{\cdot}3H_2O$ was transformed to pure white MgO powder (Figure 4e, f), suggesting that the small amount of unremoved dye on $MgCO_3{\cdot}3H_2O$ was almost completely decomposed.

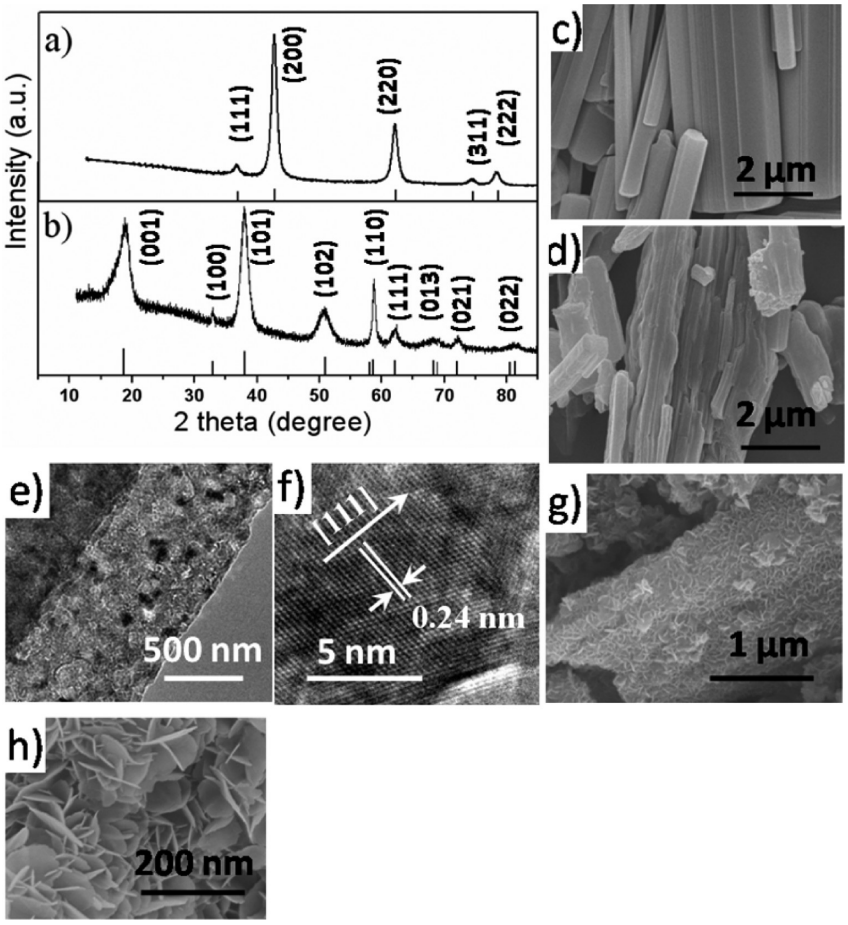

Figure 1. XRD patterns for the (a) $MgO_{600-1.5h}$ obtained by heating $MgCO_3{\cdot}3H_2O$ at 600 °C for 1.5h and (b) pure $Mg(OH)_2$ phase obtained after 1 h hydration of $MgO_{600-1.5h}$ in 2.5 mg L^{-1} AB solution at room temperature for 1 h. SEM images for (c) $MgCO_3{\cdot}3H_2O$ microrods, (d) porous MgO microrods, and (g, h) $Mg(OH)_2$ micro/nanorods. (e, f) TEM images for porous MgO microrods.

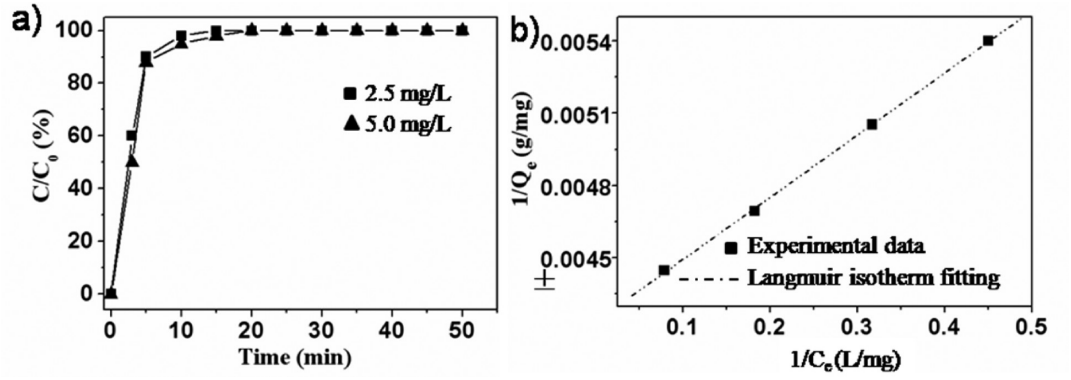

Figure 2. (a) Dye removal efficiency using 1 g/L $Mg(OH)_2$. The concentrations of the AB solutions were 2.5 (▰) and 5.0 (■) mg/L, respectively. (b) the adsorption isotherm of AB on the $Mg(OH)_2$ adsorbent.

Experiments were conducted to determine whether the recovered $Mg(OH)_2$ could still maintain the adsorption capacity for low concentrations of AB solutions in the repeating cycles. Both XRD patterns and SEM images revealed that the recovered $Mg(OH)_2$ could still hold the initial phase, size, and morphology after readsorption/redesorption experiments (see Figure S4 in the Supporting Information). It showed that the recovered $Mg(OH)_2$ still possessed high adsorption capacity close to that of the initial $Mg(OH)_2$ adsorbent (see Figure S5 in the Supporting Information). Moreover, the removal efficiency of the $Mg(OH)_2$ nanoadsorbent constantly maintained at a high level in five continuous cycles, and the enrichment multiples of dyes remained more than 4000 times during these processes. These results suggested that the $Mg(OH)_2$ adsorbent was stable and reusable for multiple cycles.

The enriched dye solution at a high concentration of more than 20 000 mg/L corresponds to a 4000-fold enrichment, which is promising for direct use in the practical scenarios. We speculate the reason for the higher adsorption rate and capacity

dx.doi.org/10.1021/am402374e | ACS Appl. Mater. Interfaces 2013, 5, 7698−7703

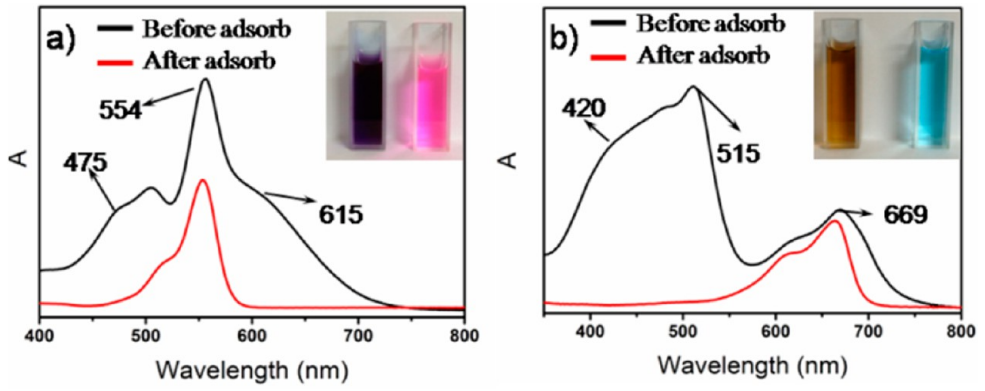

Figure 3. UV spectra of (a) dye solution **1** containing Orange G (anionic, 10 mg/L), Rhodamine B (cationic, 5 mg/L), and Coomassie Brilliant Blue R-250 (anionic, 10 mg/L); and (b) solution **2** containing orange IV (anionic, 15 mg/L), eosin B (anionic, 5 mg/L), and methylene blue (cationic, 5 mg/L) before and after adsorption. The inset shows the photos of the dye solution before (left) and after (right) adsorption.

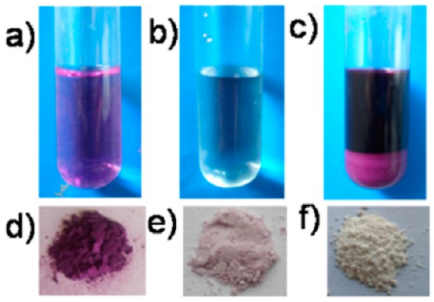

Figure 4. Preconcentration test for the dilute AB solution: (a) AB solution with a concentration of 5 mg/L and (b) colorless solution decolored by the $Mg(OH)_2$ adosrbent. (c) Enriched AB dye solution with the concentration of ~20.1 g/L . (d) Dye-loaded $Mg(OH)_2$ powder, (e) dye-free $MgCO_3{\cdot}3H_2O$ powder. (f) MgO powder regenerated from $MgCO_3{\cdot}3H_2O$ as shown in e.

may be related to the structure of the hydration precursor. Therefore, the influence of the MgO precursor to the adsorption behavior of the $Mg(OH)_2$ adsorbent was investigated. Table 1 shows the adsorption performances of three $Mg(OH)_2$ adsorbents derived from different MgO precursors. The MgO precursors were obtained by heating $MgCO_3{\cdot}3H_2O$ at 600 °C for 1.5, 3 , and 12 h, respectively. It revealed that longer heating time led to the increase of the primary particles size of MgO. The phase contents of $Mg(OH)_2$ after 0.5 h hydration for $MgO_{600-1.5h}$, MgO_{600-3h}, $MgO_{600-12h}$ were 69, 28, and 12%, respectively, indicating that small particle size could facilitate fast hydration of MgO. Moreover, the dye removal rate was found to depend on the hydration speed. The $Mg(OH)_{2\ 600-1.5h}$ exhibited the highest dye removal rate. The adsorption isotherms revealed that the saturated adsorption capacity for the $Mg(OH)_{2\ 600-12h}$ was only 52 mg/g, which accounted for ~1/3 of $Mg(OH)_{2\ 600-1.5h}$. These results indicated that more crystalline MgO resulted in lower dye removal rate and lower adsorption capacity of the $Mg(OH)_2$.

Another superiority of the strategy is its selectivity toward anionic dyes. It has been reported in the literature that $Mg(OH)_2$ exhibited relatively high adsorption efficiency to the anionic pollutants. The selectivity might be due to the electrostatic attraction between the negatively charged and $Mg(OH)_2$ surface. However, it was found that the surface charges of $Mg(OH)_2$ obtained by different methods could vary considerably.[22] To further explore the adsorption mechanism of the $Mg(OH)_2$ micro/nanorods, Zeta potential was measured during the hydration process. As show in Figure 5, upon the addition of MgO in pure water, the pH value increased shortly to ~10.6. Meanwhile, the zeta potential increased to 12.0. After 10 min, the zeta potential reached to the maximum value of 14.4, and the pH value decreased further to ~10.4. As time proceeded, the zeta potential gradually decreased and reached a minimum value of 4.39, whereas the pH value remained unchanged. Therefore, it was possibly the electrostatic interaction that caused the selective adsorption. However, the decreasing zeta potential with time was hard to explain. The mechanism might be more complicated because the whole process involved two reactions, the hydration of MgO and adsorption of the anions.

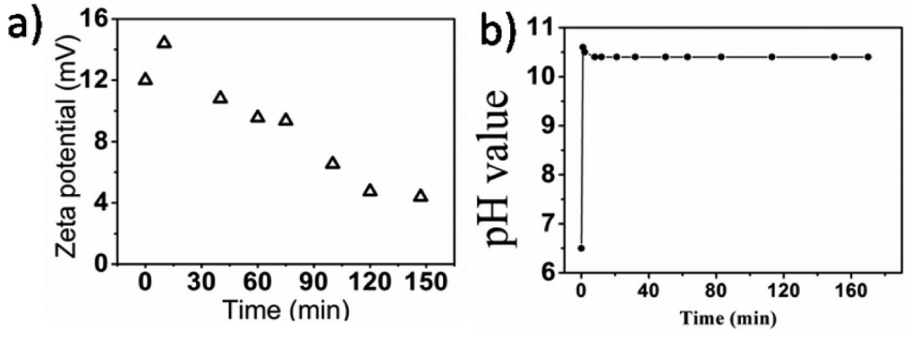

Figure 5. (a) Zeta potential and (b) the coresponding pH value determined during the adsorption process.

4. CONCLUSIONS

In conclusion, a new strategy was developed to enrich wastewater containing dilute anionic dyes. $Mg(OH)_2$ micro/nanorods that derived from MgO mesoporous rod showed high adsorption capacity to the anionic dyes. On the basis of the reversible phase transformation from a highly adsorptive nano-$Mg(OH)_2$ aggregate to bulk $MgCO_3{\cdot}3H_2O$, retrieval of the dyes were achieved. The concentration of the final dye solution could reach to ~20000 mg/L, which is nearly ~4000-fold enrichment of the dilute dye wastewater (5 mg/L). The strategy proposed in this work may also be extended to the disposal of other organic wastes that contain anionic functional groups.

■ ASSOCIATED CONTENT

Supporting Information

The structure details of MgO microrods, the kinetics modeling of the adsorption process, the structure of the regenerated $Mg(OH)_2$ adsorbent, and cycling performance of the adsorbent. This material is available free of charge via the Internet at http://pubs.acs.org.

■ AUTHOR INFORMATION

Corresponding Author

*E-mail: zlin@fjirsm.ac.cn. Tel: (+86)-591-83705445. Fax: (+86)-591-83705445.

Notes

The authors declare no competing financial interest.

■ ACKNOWLEDGMENTS

This work was funded by National Basic Research Program of China (973 Program) (2010CB933501, 2013CB934302), the Outstanding Youth Fund (21125730), the National Natural Science Foundation of China (21273237, 21103191), Fund of Fujian Key Laboratory of Nanomaterials (2006L2005), the Knowledge Innovation Program of the Chinese Academy of Sciences (KJCX2-YW-N50, KJCX2-EW-J02)

■ REFERENCES

(1) Ma, L. M.; Zhang, W. X. *Environ. Sci. Technol.* **2008**, *42*, 5384−5389.
(2) Parsons, S. A.; Jefferson, B.; *Introduction to Potable Water Treatment Processes*; Blackwell Publishing: Oxford, U.K., 2006; Vol. 3, p 26.
(3) Stephenson, R. J.; Duff S., J. B. *Water Res.* **1996**, *30*, 781−792.
(4) Chiou, M. S.; Chuang, G. S. *Chemosphere* **2006**, *62*, 731−740.
(5) Tang, J. W.; Zou, Z. G.; Ye, J. H. *Angew. Chem., Int. Ed.* **2004**, *43*, 4463−4466.
(6) Zhao, L.; Chen, X. F.; Wang, X. C.; Zhang, Y. J.; Wei, W.; Sun, Y. H.; Antonietti, M.; Titirici, M. M. *Adv. Mater.* **2010**, *22*, 3317−3321.
(7) Guo, X.; Fei, G. T.; Su, H.; Zhang, L. D. *J. Mater. Chem.* **2011**, *21*, 8618−8625.
(8) Saxe, J. P.; Lubenow, B. L.; Chiu, P. C.; Huang, C. P.; Cha, D. K. *Water Environ. Res.* **2006**, *78* (1), 19−25.
(9) Al-Degs, Y.; Khraisheh, M. A. M.; Allen, S. J.; Ahmad, M. N.; Walker, G. M. *Chem. Eng. J.* **2007**, *128*, 163−167.
(10) Baskaralingam, P.; Pulikesi, M.; Ramamurthi, V.; Elango, D.; Ramamurthi, V.; Sivanesan, S. *J. Hazard. Mater.* **2006**, *128*, 138−144.
(11) Kyzas, G. Z.; Lazaridis, N. K.; Mitropoulos, A. C. *Chem. Eng. J.* **2012**, *189−190*, 148−159.
(12) Yu, X. Y.; Luo, T.; Jia, Y.; Xu, R. X.; Gao, C.; Zhang, Y. X.; Liu, J. H.; Huang, X. J. *Nanoscale* **2012**, *4*, 3466−3474.
(13) Liu, W. Z.; Huang, F.; Liao, Y. Q.; Zhang, J.; Ren, G. Q.; Zhuang, Z. Y.; Zhen, J. S.; Lin, Z.; Wang, C. *Angew. Chem., Int. Ed.* **2008**, *47*, 5619−5622.
(14) Wang, Y. J.; Chen, D. G.; Wang, Y. D.; Huang, F.; Hu, Q. C.; Lin, Z. *Nanoscale* **2012**, *4*, 3665−3668.
(15) Liu, W. Z.; Huang, F.; Wang, Y. J.; Zou, T.; Zheng, J. S.; Lin, Z. *Environ. Sci. Technol.* **2011**, *45*, 1955−1961.
(16) Gasser, M. S.; Morad, G. H. A.; Aly, H. F. *J. .Hazard. Mater.* **2007**, *142*, 118−129.
(17) Sasaki, K.; Fukumoto, N.; Moriyama, S.; Hirajima, T. *J. Hazard. Mater.* **2011**, *191*, 240−248.
(18) Gao, B. Y.; Yue, Q. Y.; Wang, Y.; Zhou, W. Z. *J. Environ. Manage.* **2007**, *82*, 167−172.
(19) Ecker, M. *Purification of liquids, especially water containing heavy metal ions, involves bonding the impurities on or in magnesium hydroxide.* DE 10318746-A1, 2004.
(20) Wang, Y. J.; Liu, W. Z.; Zou, T.; Lin, Z. *CrystEngComm* **2012**, *14*, 7165−7169.
(21) Langmuir, I. *J. Am. Chem. Soc.* **1918**, *40*, 1361−1403.
(22) Pan, X. H.; Wang, Y. H.; Chen, Z.; Pan, D. M.; Cheng, Y. J.; Liu, Z. J.; Lin, Z.; Guan, X. *ACS Appl. Mater. Interfaces* **2013**, *5*, 1137−1142.